EUROPEAN ORGANIZATION FOR NUCLEAR RESEARCH

CERN-PPE/96-165
26th November, 1996

Hyperon Production in Proton–Sulphur Collisions at 200 GeV/c.

The WA94 Collaboration

S. Abatzis[1], E. Andersen[3], A. Andrighetto[11], F. Antinori[6], A.C. Bayes[4], M. Benayoun[7], W. Beusch[6], J. Böhm[8], J.N. Carney[4], N. Carrer[11], B. de la Cruz[10], J.P. Davies[4], D. Di Bari[2], D. Elia[2], D. Evans[4], K. Fanebust[3], R.A. Fini[2], B.R. French[6], J. Ftáčnik[5], B. Ghidini[2], H. Helstrup[3], A.K. Holme[6], A. Jacholkowski[2], J. Kahane[7], V.A. Katchanov[12], J.B. Kinson[4], A. Kirk[4], K. Knudson[6], I. Králik[8], P. Ladrón de Guevara[10], J.C. Lassalle[6], V. Lenti[2], Ph. Leruste[7], R. Lietava[5], R.A. Loconsole[2], G. Løvhøiden[3], V. Manzari[2], M. Morando[11], J.L. Narjoux[7], F. Navach[2], K.L. Norman[4], F. Pellegrini[11], E. Quercigh[6], R.A. Ricci[9], K. Šafařík[6], L. Šándor[8], G. Segato[11], M. Sené[7], R. Sené[7], P. Sennels[3], A.V. Singovski[12], T.F. Thorsteinsen[3], J. Urbán[8], G. Vassiliadis[1], M. Venables[4], O. Villalobos Baillie[4], A. Volte[7], M.F. Votruba[4], and P. Závada[8].

Abstract

The WA94 experiment uses the production of strange particles and antiparticles to investigate the properties of hot hadronic matter created in heavy–ion interactions. Λ, $\overline{\Lambda}$, Ξ^- and $\overline{\Xi}^+$ particle yields and transverse mass spectra are presented for pS interactions. These results are compared with those from SS interactions. Our results are also compared with those from pW and SW interactions of the WA85 experiment.

[1] Athens University, Athens, Greece.
[2] Università di Bari and Sezione INFN, Bari, Italy.
[3] Universitetet i Bergen, Bergen, Norway.
[4] University of Birmingham, Birmingham, U.K.
[5] Comenius University, Bratislava, Slovakia.

[6] CERN, Geneva, Switzerland.
[7] Collège de France and IN2P3, Paris, France.
[8] Institute of Experimental Physics, Košice, Slovakia.
[9] Laboratorio Nazionale di Legnaro, Legnaro, Italy.
[10] CIEMAT, Madrid, Spain.
[11] Dipartimento di Fisica dell'Università and Sezione INFN, Padua, Italy.
[12] IHEP, Protvino, Russia

To be submitted to Physics Letters B

In order to improve understanding of the dynamics of hot, hadronic matter, the WA94 experiment examines hyperon production from collisions of ultra–relativistic nuclei. Current understanding suggests that hyperons provide a test for the existence of a Quark–Gluon Plasma (QGP) [**?**], which might be formed in ultra–relativistic heavy–ion collisions. In the simplest case, the central region of such collisions is thought to exist in one of two states; a dense hadron gas (HG) phase or a QGP phase. Both produce strangeness and both can saturate strangeness phase space. The QGP phase achieves saturation much earlier than the HG phase, because low threshold $s\bar{s}$ production from gluon-gluon fusion is open to it. This gives rise to copious production of strange quarks and anti-quarks compared with the HG scenario in a short-lived fireball [**?**, **?**]. It has been argued, therefore, that relative abundances of particles containing different amount of strangeness, such as Ξ^-/Λ and especially $\overline{\Xi}^+/\overline{\Lambda}$, could be sensitive to a phase change [**?**]. For this reason, the WA94 experiment examines sulphur–sulphur interactions with the aim of measuring strangeness enhancement, using proton–sulphur interactions as a control. It is also possible to gain independent estimates of temperature and to investigate collective flow from transverse mass spectra.

The WA94 experiment [**?**] was performed at the CERN OMEGA spectrometer and took data using both a sulphur ion beam and a proton beam incident upon a sulphur target. Figure **??** shows the layout for the proton beam run. Scintillators and differential Čerenkov counters (CEDARS [**?**]) upstream of the target identified an incident proton. A further scintillator, in anti-coincidence with the beam scintillators, was positioned on the beam line, downstream from the target, to detect the presence of a beam proton that had not interacted with a target nucleus. Multiwire Proportional Chambers (MWPCs), operating in 'butterfly' mode [**?**], provided tracking information. Their positions, relative to the 9% interaction length target, ensured that only particles in the kinematic region $p_{\mathrm{T}} \geq 0.6$ GeV/c and $2.4 < Y_{\mathrm{LAB}} < 3.2$ were selected. This corresponds to the central rapidity region for the sulphur beam run and is similar to the centre–of–mass rapidity coverage used by WA85 for sulphur–tungsten and proton–tungsten interactions [**?**].

To enhance the number of events with a medium p_{T} track, the scintillator hodoscopes HZ0 and HZ1 were placed downstream from the MWPCs. Each half of a hodoscope consisted of five horizontal slabs, covering the same phase space as the MWPCs. As the magnetic field was aligned along the vertical axis, positively and negatively charged tracks traced through different halves of the hodoscopes. Only events in which at least one track satisfied a correlation of hits in either the left– or right–hand halves of the hodoscopes were considered. A further trigger condition, to increase V^0 detection, required a multiplicity greater than one in the fourth MWPC and also in at least two of the first three MWPCs. The apparatus

was symmetric with respect to charge, giving equal acceptances for both particles and anti–particles and data were taken with both magnetic field polarities so as to reduce residual systematic effects. The strange particle sample was taken from a total of 52 million triggers.

The selection procedure for V^0s and cascades is very similar to that employed by WA94 in sulphur–sulphur interactions [**?**], taking into account the small differences in layout. A pair of oppositely–charged tracks is considered as a Λ or $\overline{\Lambda}$ candidate if

1. each track has at least four space points,
2. each track traces through the seven MWPCs,
3. the distance of closest approach between the two tracks is less than 1.0 cm,
4. the angle between the V^0 line–of–flight from the target and the sum of the tracks' three-momenta is less than $0.75°$, ensuring that the candidate comes from the target,
5. the decay occurs between 135 cm from the target and the first MWPC,
6. the Podolanski–Armenteros variable α [**?**] lies in the range $0.45 < |\alpha| < 0.60$, reducing contamination from K^0 decays[1],
7. the transverse momentum of the decay tracks with respect to the V^0 is greater than 0.01 GeV/c, to remove background from photon conversions, and
8. at least one of the decay tracks satisfies the hodoscope condition.

Figures **??**a and **??**b show the $(p\pi^-)$ and $(\overline{p}\pi^+)$ mass spectra that these criteria yield. The vertical lines indicate a 50 MeV interval centred on the Λ mass, giving 11846 Λ and 3147 $\overline{\Lambda}$ candidates.The shaded regions are those candidates whose mass, when interpreted as $(\pi^+\pi^-)$, lie within 50 MeV of the K^0 mass. Figure **??** shows the Λ candidates' masses when interpreted as $(\overline{p}\pi^-)$ and $(\pi^+\pi^-)$. The vertical lines show again a 50 MeV region centred on the $\overline{\Lambda}$ mass. From this plot, it can be shown that there is about 2% contamination in the $\overline{\Lambda}$ sample from K^0s.

The Ξ^- and $\overline{\Xi}^+$ candidates are selected by combining a V^0 with an appropriately charged pion to identify the decay sequence

[1] This is equivalent to a cut of $\cos\theta^* \leq -0.5$, where $\cos\theta^*$ is the angle between the lines of flight of the baryon in the V^0 rest frame and of the V^0 in the LAB frame. Positive α corresponds to Λ and negative α corresponds to $\overline{\Lambda}$.

$$\begin{array}{lcccc} \Xi^- & \rightarrow & \Lambda & + & \pi^- \\ & & \downarrow & & \\ & & \mathrm{p} & + & \pi^- \end{array}$$

or the charge conjugate decay. Any combination of a V^0 with an appropriately charged pion is considered as a cascade candidate if

1. each track has at least four space points,
2. each track traces through the first four MWPCs,
3. the distance of closest approach between the line of flight of the V^0 and the pion is less than 1.6 cm,
4. the cascade decay occurs between 90 cm from the target and the first MWPC,
5. the impact parameter of the cascade in the target plane is less than 2.0 cm (the cascade comes from the target),
6. the impact parameter of the pion from the cascade vertex, in the target plane, is greater than 6.0 cm (the pion does not come from the target),
7. the V^0 vertex is downstream from the cascade vertex, and
8. at least one of the tracks satisfies the hodoscope condition.

Figures **??**c and **??**d show the mass distributions from the resulting Ξ^- and $\overline{\Xi}^+$ candidates. There are clear peaks with little background at the Ξ mass. The vertical lines indicate a 100 MeV interval centred on the Ξ^- mass, giving 450 Ξ^- and 185 $\overline{\Xi}^+$ candidates.

The data have been corrected for geometrical acceptance, unseen decay modes and reconstruction efficiencies. A further correction, for the contamination of the Λ and $\overline{\Lambda}$ samples due to feed–down from Ξ^- and Ξ^0 decays, has been made. It has been found that 16% of the Λ sample and 28% of the $\overline{\Lambda}$ sample come from these decays. Figure **??** shows the corrected transverse mass distributions, which have been fitted using the expression [**?**]

$$\frac{1}{m_{\mathrm{T}}^{3/2}}\frac{\mathrm{d}N}{\mathrm{d}m_{\mathrm{T}}} = Ae^{-m_{\mathrm{T}}/\tau},$$

where $m_{\mathrm{T}} = \sqrt{p_{\mathrm{T}}^2 + m^2}$ is the transverse mass, in the rapidity window $2.5 < Y_{\mathrm{LAB}} < 3.0$. The inverse slopes are presented in table 1, along with corresponding results for the WA94 sulphur–sulphur data [**?**]. The errors on the inverse slopes are statistical only. The systematic errors are estimated to be about 10 MeV. Each proton–sulphur inverse slope is smaller than that for the corresponding

sulphur–sulphur inverse slope. It is interesting to note that the WA85 experiment reports a similar relationship between proton– and sulphur–induced collisions in a similar rapidity window [**?**, **?**].

Table 2 shows relative hyperon yields for the rapidity interval $2.5 < Y_{\rm LAB} < 3.0$ for both proton–sulphur and sulphur–sulphur collisions. The regions $1.2 < p_{\rm T} < 3.0$ GeV/c and $m_{\rm T} \geq 1.9$ GeV correspond to where Ξ^- and Λ acceptances overlap. Ratios for the interval $1.0 < p_{\rm T} < 2.0$ GeV/c are extrapolated from the $1.2 < p_{\rm T} < 3.0$ GeV/c region and are shown in table 2 and in figure **??** to allow direct comparison with the $\overline{\Xi}^+/\overline{\Lambda}$ ratio from proton–proton collisions obtained by the AFS collaboration (0.06 ± 0.02) [**?**]. The $\overline{\Lambda}/\Lambda$ and $\overline{\Xi}^+/\Xi^-$ ratios for proton–sulphur collisions are consistent with the corresponding ratios from sulphur–sulphur collisions. There is, however, a 30% increase in the $\overline{\Xi}^+/\overline{\Lambda}$ ratio when going from proton– to sulphur–induced collisions. This corresponds to about a two standard deviation effect. The WA85 experiment observed a similar effect when going from proton–tungsten to sulphur–tungsten collisions, albeit in a slightly different kinematic window [**?**, **?**].

In conclusion, results are presented for hyperon production from proton–sulphur interactions at 200 GeV/c. They have been compared with the WA94 sulphur–sulphur results in the same laboratory kinematic window. The inverse slopes obtained from the transverse mass distributions for Λ, $\overline{\Lambda}$, Ξ^- and $\overline{\Xi}^+$ decays are lower than those obtained from the sulphur beam data. The relative hyperon yields have also been determined. The $\overline{\Lambda}/\Lambda$ and $\overline{\Xi}^+/\Xi^-$ ratios for proton–sulphur collisions are consistent with the corresponding ratios from sulphur–sulphur collisions. There is a 30% increase in the $\overline{\Xi}^+/\overline{\Lambda}$ ratio when going from proton– to sulphur–induced collisions.

References

[1] J. Rafelski and B. Müller, Phys. Rev. Lett. **48** (1982) 1066.

[2] P. Koch, B. Müller and J. Rafelski, Phys. Rep. **142** (1986) 167.

[3] E. Schnedermann and U. Heinz, Phys. Rev. Lett. **69** (1992) 2908.

[4] J. Rafelski, Phys. Lett. **B262** (1991) 333.

[5] WA94 proposal, CERN/SPSLC/91-5 P257 (1991).

[6] *The CEDAR counters for Particle Identification in the SPS Secondary Beams: A Description and an Operation Manual*, C. Bovet *et al.*, CERN 82-13 (1982).

[7] W. Beusch *et al.*, Nucl. Inst. and Meth. **A249** (1986) 391.

[8] WA85 Proposal, CERN/SPSLC/84-76 P206 (1984).

[9] S.Abatzis *et al.*, Phys. Lett. **B354** (1995) 178.

[10] J. Podolanski and R. Armenteros, Phil. Mag **45** (1954) 13.

[11] H. C. Eggers and J. Rafelski, Int. J. Mod. Phys. **A6** (1991) 1067.

[12] Thesis of J. P. Davies, *Production of Strange Particles in Ultra-Relativistic Proton-Tungsten Collisions at 200 GeV/c*, The University of Birmingham (1995).

[13] S.Abatzis *et al.*, Phys. Lett. **B359** (1995) 382.

[14] T. Åkesson *et al.*, Nucl. Phys. **B354** (1984) 1.

[15] J. P. Davies *et al.*, Proceedings of Strangeness '95, Tucson, Arizona, AIP Press (1995) 223.

[16] D. Evans *et al.*, Proceedings of Strangeness '95, Tucson, Arizona, AIP Press (1995) 234.

Tables

Table 1: Inverse slopes of hyperons in proton–sulphur and sulphur–sulphur interactions.

Particle	Inverse slope (MeV)	
	Proton Interactions	Sulphur Interactions
Λ	191 ± 3	213 ± 2
$\overline{\Lambda}$	181 ± 5	204 ± 5
Ξ^-	212 ± 9	222 ± 10
$\overline{\Xi}^+$	202 ± 12	208 ± 25

Table 2: Relative hyperon yields in proton–sulphur and sulphur–sulphur interactions.

Ratio	$2.5 \leq Y_{\mathrm{LAB}} \leq 3.0$, $m_{\mathrm{T}} \geq 1.9$ GeV	
	Proton Interaction	Sulphur Interaction
$\overline{\Lambda}/\Lambda$	0.20 ± 0.01	0.22 ± 0.01
$\overline{\Xi}^{+}/\Xi^{-}$	0.43 ± 0.05	0.54 ± 0.06
Ξ^{-}/Λ	0.15 ± 0.01	0.18 ± 0.01
$\overline{\Xi}^{+}/\overline{\Lambda}$	0.30 ± 0.03	0.44 ± 0.02

Ratio	$2.5 \leq Y_{\mathrm{LAB}} \leq 3.0$, $1.2 \leq p_{\mathrm{T}} \leq 3.0$ GeV/c	
	Proton Interaction	Sulphur Interaction
$\overline{\Lambda}/\Lambda$	0.22 ± 0.01	0.23 ± 0.01
$\overline{\Xi}^{+}/\Xi^{-}$	0.46 ± 0.05	0.55 ± 0.07
Ξ^{-}/Λ	0.078 ± 0.004	0.09 ± 0.01
$\overline{\Xi}^{+}/\overline{\Lambda}$	0.16 ± 0.02	0.21 ± 0.02

Ratio	$2.5 \leq Y_{\mathrm{LAB}} \leq 3.0$, $1.0 \leq p_{\mathrm{T}} \leq 2.0$ GeV/c	
	Proton Interaction	Sulphur Interaction
$\overline{\Lambda}/\Lambda$	0.24 ± 0.01	0.24 ± 0.01
$\overline{\Xi}^{+}/\Xi^{-}$	0.45 ± 0.06	0.58 ± 0.07
Ξ^{-}/Λ	0.068 ± 0.007	0.08 ± 0.01
$\overline{\Xi}^{+}/\overline{\Lambda}$	0.13 ± 0.02	0.20 ± 0.02

Figures

Figure 1: Layout of the WA94 experiment as used for proton–sulphur data taking.

Figure 2: Effective mass distributions for a) $p\pi^-$, b) $\overline{p}\pi^+$, c) $\Lambda\pi^-$, and d) $\overline{\Lambda}\pi^+$.

Figure 3: Effective mass of $\pi^+\pi^-$ versus effective mass of $p\pi^-$ for Λ candidates.

Figure 4: Transverse mass distributions for a) Λ and $\overline{\Lambda}$ and b) Ξ^- and $\overline{\Xi}^+$.

Figure 5: Comparison of WA94 Ξ^-/Λ and $\overline{\Xi}^+/\overline{\Lambda}$ ratios with WA85 and AFS ratios.

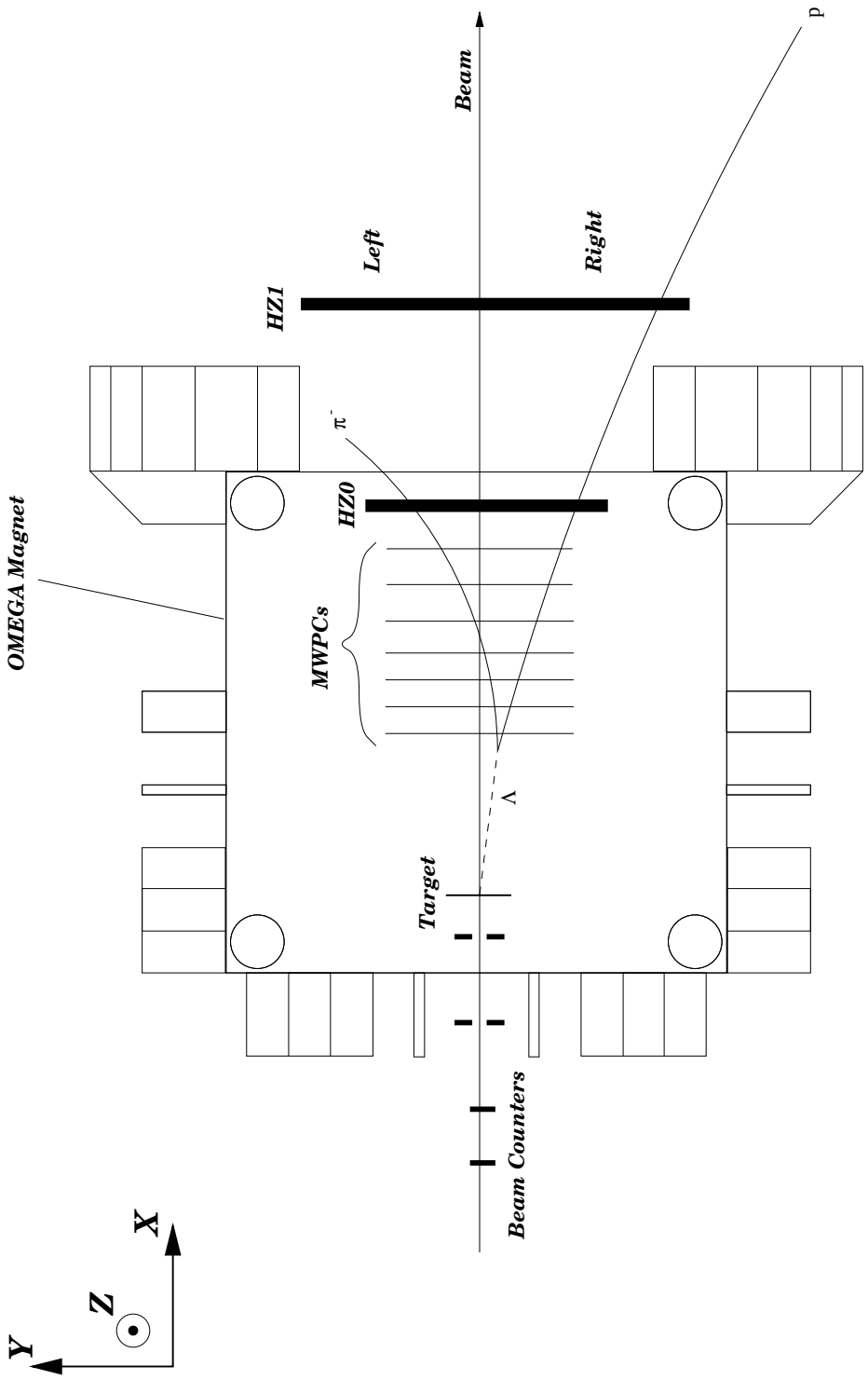
Beam
p
Left
Right
HZ1
π-
HZ0
OMEGA Magnet
MWPCs
Λ
Target
Beam Counters
X
Z
Y

Figure 1:

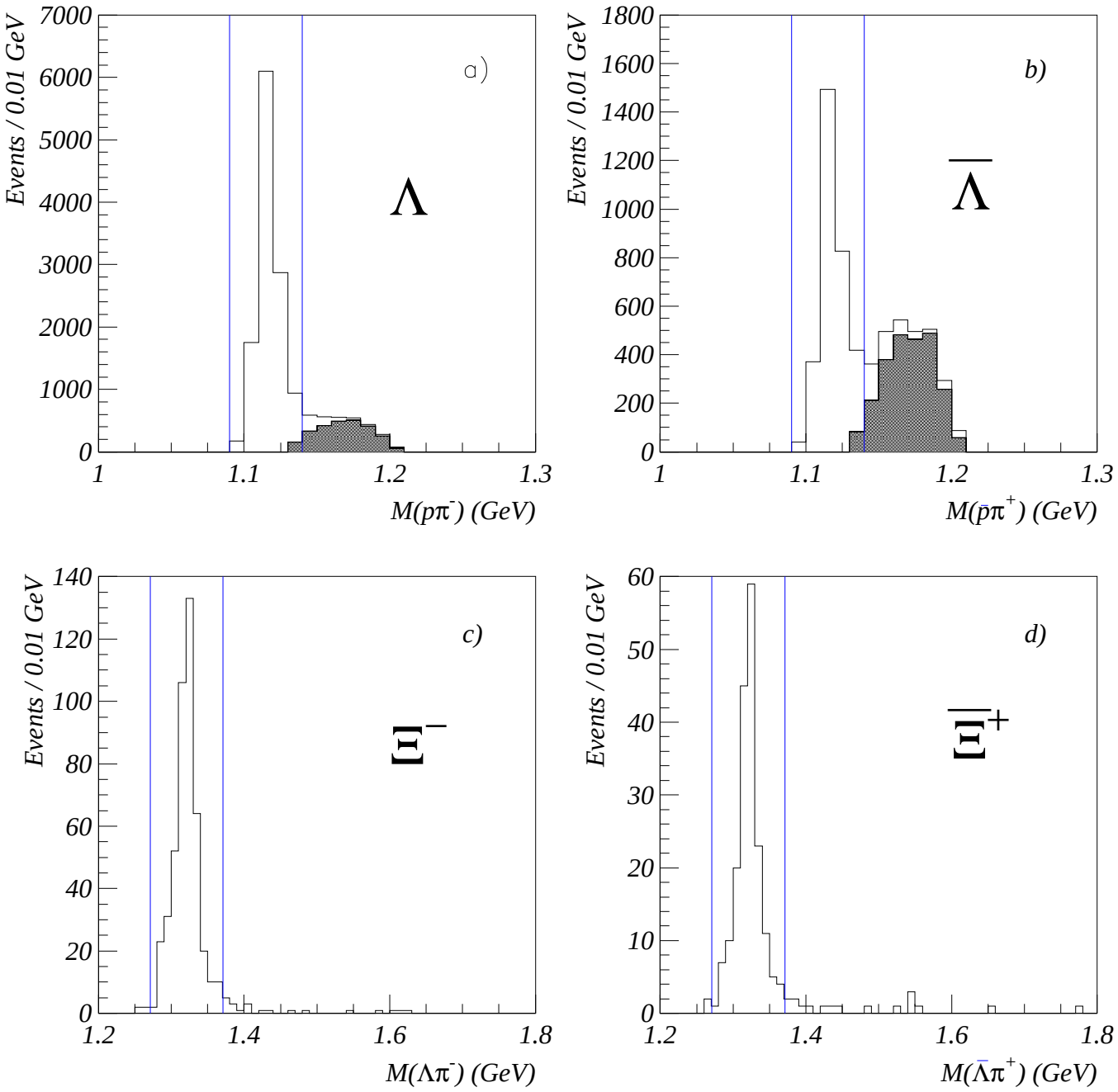
a)
Λ
Events / 0.01 GeV
M(pπ⁻) (GeV)
b)
Λ̄
Events / 0.01 GeV
M(p̄π⁺) (GeV)
c)
Ξ⁻
Events / 0.01 GeV
M(Λπ⁻) (GeV)
d)
Ξ̄⁺
Events / 0.01 GeV
M(Λ̄π⁺) (GeV)

Figure 2:

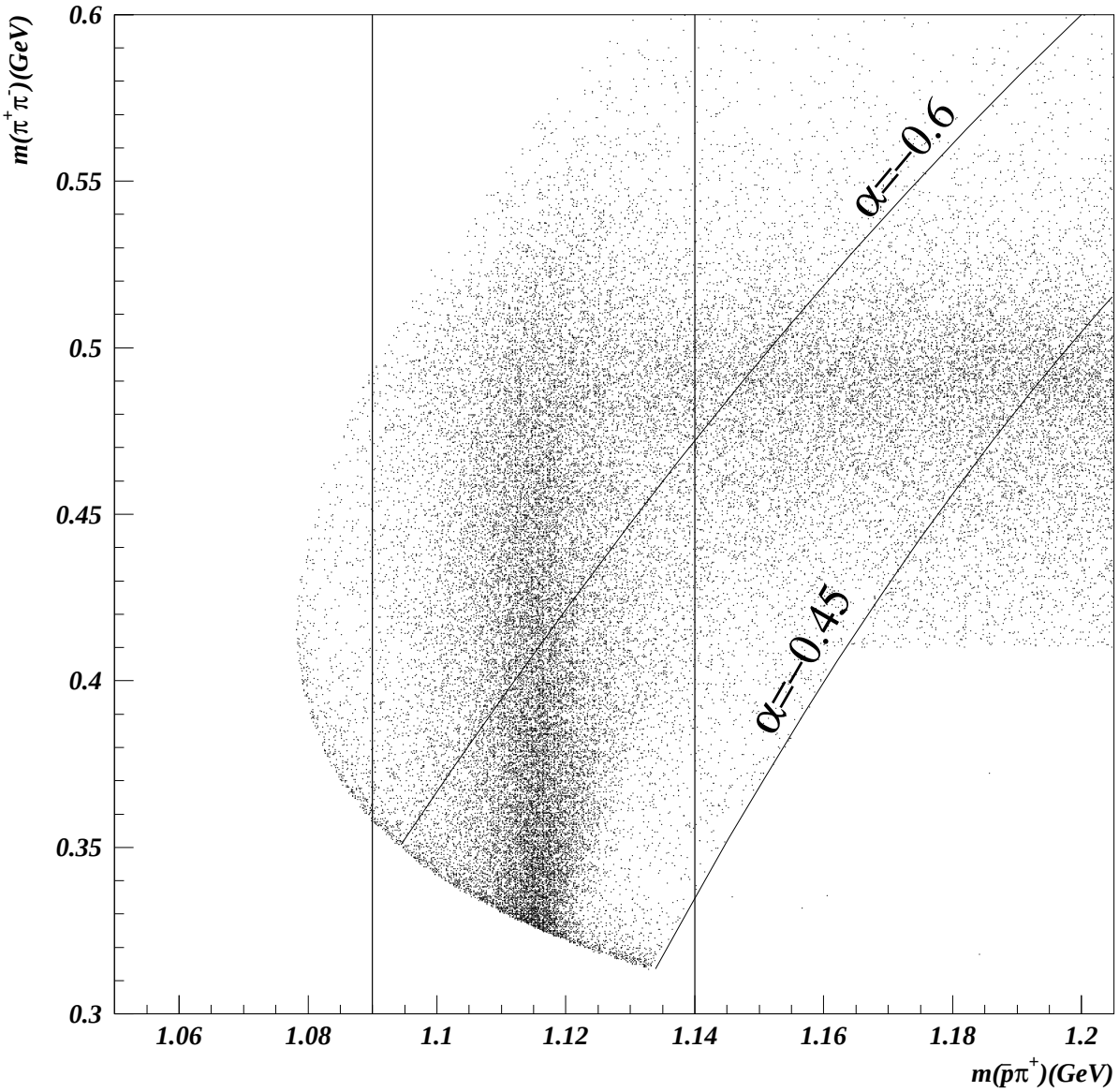
0.6
0.55
0.5
0.45
0.4
0.35
0.3
m(π⁺π⁻)(GeV)
1.06
1.08
1.1
1.12
1.14
1.16
1.18
1.2
m(p̄π⁺)(GeV)
α=−0.6
α=−0.45

Figure 3:

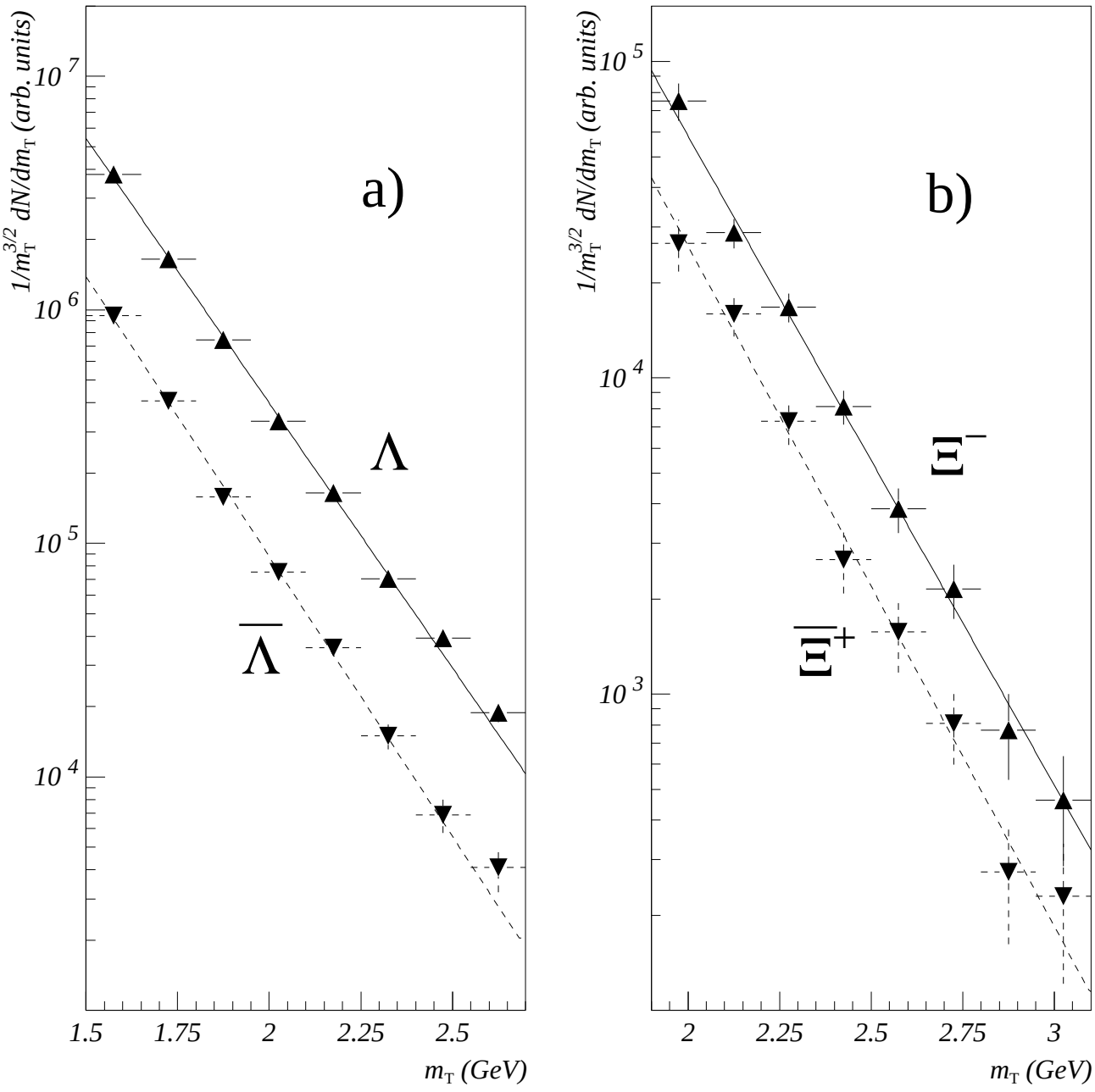
a)
b)
$1/m_T^{3/2}\, dN/dm_T$ (arb. units)
m_T (GeV)
Λ
$\overline{\Lambda}$
Ξ^-
$\overline{\Xi}^+$

Figure 4:

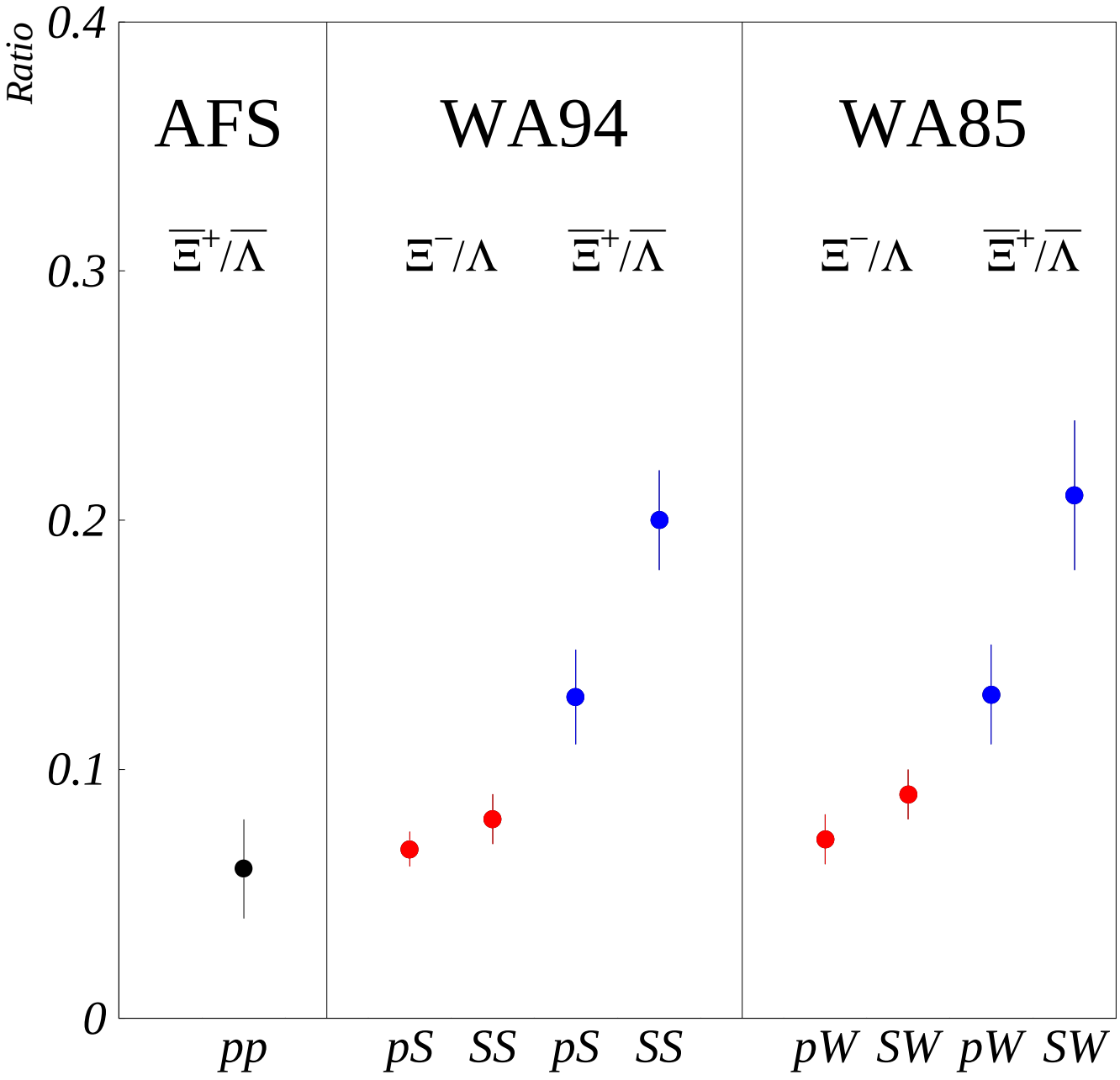
Ratio
0.4
0.3
0.2
0.1
0
AFS
WA94
WA85
$\overline{\Xi}^+/\overline{\Lambda}$
Ξ^-/Λ
$\overline{\Xi}^+/\overline{\Lambda}$
Ξ^-/Λ
$\overline{\Xi}^+/\overline{\Lambda}$
pp
pS
SS
pS
SS
pW
SW
pW
SW

Figure 5: